Published in final edited form as:
Epilepsia. 2014 February ; 55(2): 256–263. doi:10.1111/epi.12486.

Differences in Paracingulate Connectivity Associated with Epileptiform Discharges and Uncontrolled Seizures in Genetic Generalized Epilepsy

Benjamin P Kay, PhD[1,2], **Scott K Holland, PhD**[2], **Michael D Privitera, MD**[3], and **Jerzy P Szaflarski, MD, PhD**[3,4]

[1]Neuroscience Graduate Program, University of Cincinnati, Cincinnati, OH

[2]Pediatric Neuroimaging Research Consortium, Cincinnati Children's Hospital Medical Center, Cincinnati, OH

[3]Department of Neurology and the Cincinnati Epilepsy Center, University of Cincinnati, Cincinnati, OH

[4]Department of Neurology and the UAB Epilepsy Center, University of Alabama at Birmingham, Birmingham, AL

Summary

Objective—Patients with genetic generalized epilepsy (GGE) frequently continue to suffer from seizures despite appropriate clinical management. GGE is associated with changes in the resting-state networks modulated by clinical factors such as duration of disease and response to treatment. However, the effect of GSWDs and/or seizures on resting-state functional connectivity (RSFC) is not well understood.

Methods—We investigated the effects of GSWD frequency (in GGE patients), GGE (patients vs. healthy controls), and seizures (uncontrolled vs. controlled) on RSFC using seed-based voxel correlation in simultaneous EEG and resting-state fMRI (EEG/fMRI) data from 72 GGE patients (23 w/uncontrolled seizures) and 38 healthy controls. We used seeds in paracingulate cortex, thalamus, cerebellum, and posterior cingulate cortex to examine changes in cortical-subcortical resting-state networks and the default mode network (DMN). We excluded from analyses time points surrounding GSWDs to avoid possible contamination of the resting state.

Results—(1) Higher frequency of GSWDs was associated with an increase in seed-based voxel correlation with cortical and subcortical brain regions associated with executive function, attention, and the DMN, (2) RSFC in patients with GGE, when compared to healthy controls, was increased between paracingulate cortex and anterior, but not posterior, thalamus, and (3) GGE patients with uncontrolled seizures exhibited decreased cereballar RSFC.

Corresponding Author: Benjamin P Kay University of Cincinnati Academic Health Center Graduate Program in Neuroscience 260 Stetson Street, Suite 2300 Cincinnati, OH, USA, 45267-0525 Phone: 01-513-803-0419 benjamin@benkay.net.

Disclosures

None of the authors has any conflict of interest to disclose. We confirm that we have read the Journal's position on issues involved in ethical publication and affirm that this report is consistent with those guidelines.

Significance—Our findings in this large sample of patients with GGE (1) demonstrate an effect of interictal GSWDs on resting-state networks, (2) provide evidence that different thalamic nuclei may be affected differently by GGE, and (3) suggest that cerebellum is a modulator of ictogenic circuits.

Keywords

Default Mode Network; Resting-State Functional Connectivity; Generalized Spike and Wave Discharges; Cerebellum; Thalamus; Basal Ganglia

Introduction

Genetic generalized epilepsy (GGE, formerly known as idiopathic generalized epilepsy, IGE) is a seizure disorder of presumed genetic etiology[1] that affects all age groups and accounts for 15-30% of all epilepsy cases.[2] More than 20% of GGE patients experience ongoing or "uncontrolled" seizures despite adequate clinical management.[3,4] GGE is typically associated with normal intelligence, but many patients exhibit specific, frontal-lobe cognitive deficits[5,6,7,8] that are compounded by the negative effects of anti-epileptic drugs (AEDs) on cognition.[9,10,11] Finally, psychiatric symptoms are common in patients with GGE who often present with comorbid attention deficit,[12] mood, and personality disorders.[13,14,15] Resting-state functional connectivity (RSFC) reflects anatomical (structural) connectivity in the brain[16] and may be more sensitive than diffusion tensor imaging (DTI) at detecting changes associated with GGE.[17] A growing body of evidence supports the notion of an interaction between functional/structural connectivity and neurological and psychiatric disorders, including evidence for the effects of epilepsy on cognitive and emotive brain networks.[18,12,19,20,21,22,11,17] Generalized spike and wave discharges (GSWDs) are a ubiquitous electroencephalographic hallmark of GGE as seen interictally and during absence and generalized tonic-clonic seizures (GTCs).[23,24] The prevailing theory of GSWD etiology posits that synchronized neuronal activity in reentrant thalamocortial circuits gives rise to generalized seizures,[25,26,27] possibly via a mechanism shared with sleep spindles.[28,29] This theory is supported by animal models of generalized epilepsies.[30] Subdural and depth electrodes provide a gold-standard of evidence in humans, but these surgical recording techniques are highly invasive and not performed routinely in patients with GGE.[31] Simultaneous electroencephalography and functional magnetic resonance imaging (EEG/fMRI) provides a noninvasive imaging modality with high spatial resolution suitable for clinical and experimental human use.[32] Studies of GGE have shown thalamic and widespread cortical GSWD-related activation consistent with the cortical-subcortical hypothesis of GSWD genesis.[33,34,35,36,37,38,39] EEG/fMRI studies have also demonstrated cortical deactivation associated with GSWDs specifically in regions corresponding to the default mode network (DMN),[33,34,35,36,37,38] a resting-state network thought to support consciousness.[40,41,42,43] GSWD-related deactivation of the DMN has been hypothesized as an explanation for absence seizure semiology[34] consistent with the network inhibition hypothesis.[44,45] Previous RSFC studies of GGE have observed reduced DMN connectivity in patients vs. controls,[20] even when EEG/fMRI is used to exclude the effect of GSWDs.[18,19] This relationship is dependent upon response to treatment[18] and the length of time (i.e. duration) for which a patient has had epilepsy[20]. The effects of GSWD

frequency on RSFC and the DMN have not, to our knowledge, been previously investigated. Therefore, in this EEG/fMRI study we use seed-based voxel correlations to investigate the effects of GSWDs, GGE, and treatment-resistance on RSFC in cortical-subcortical networks and the DMN.

Methods

This study examined a previously described cohort of 100 epilepsy patients and 40 healthy control subjects.[46,18,38] Epilepsy patients who satisfied published criteria for the diagnosis of GGE[1] were enrolled after evaluation at the Cincinnati Epilepsy Center. Diagnosis and treatment were directed by an epilepsy specialist[24] with specific inclusion and exclusion criteria published previously[38]. All participants in the study provided written informed consent for a protocol approved by the Institutional Review Boards of the University of Cincinnati and the Cincinnati Children's Hospital Medical Center. Each GGE patient underwent 1-3 consecutive 20-minute EEG/fMRI scans, and each healthy control subject underwent 1-2 consecutive scans. All patients and 20/40 control subjects listened to self-selected music during scanning to increase comfort and compliance. The effect of music-listening on resting-state data is discussed elsewhere[46] and was included as a covariate in analyses. As previously, seizure freedom (Seizures-) was defined as no seizures in the 3 months preceding the scanning session[24,38] while patients with any seizures (absence, tonic-clonic, or myoclonic) were included in the uncontrolled group (Seizures+). Evidence for seizures was obtained from personal interviews with the patient(s) by the primary neurologist/epilepsy specialist, by an interview at the time of EEG/fMRI scanning, and, in a majority of patients, by 24-72 hour ambulatory EEG.[24]

Eleven GGE patients failed to complete at least one scan due to claustrophobia (n=3), metallic artifacts (n=1), or not wanting to continue the procedure (n=7). Of the 89 GGE patients who completed scanning, 15 patients were excluded due to poor quality data and an additional 2 were excluded because a high number of GSWDs led to an ill-conditioned design matrix. All control subjects completed scanning, but 2 were excluded due to poor quality of the data. Thirty scans (28 GGE and 2 healthy controls) were excluded in total. Resting-state analysis was carried out on 231 scans from 72 GGE patients (152 scans) and 38 healthy controls (67 scans; Table 1). There was no significant difference in root mean square displacement or average motion cost between GGE patients and healthy control subjects (accounting for age and music-listening, displacement p=0.20, cost p=0.56), the Seizures+ and Seizures- patient groups (accounting for age, p=0.15, p=0.19), nor patients who were and were not taking valproate, which is associated with tremor (p=0.884, p=0.978), nor were these motion measures correlated with GSWD frequency (p=0.62, p=0.24).

EEG Acquisition & Processing

Acquisition and processing of EEG data simultaneous with fMRI was carried out as described previously[18,38] using Scan 4.3.5 software (Compumedics U.S.A., Ltd., El Paso, TX, U.S.A.). Briefly, subjects were fitted with an MRI-compatible EEG cap with electrodes arranged according to the international 10/20 system (Compumedics USA, Ltd., El Paso,

TX). Conductive gel (Quik-Gel; Compumedics Neuromedia Supplies, Charlotte, NC, U.S.A.) was used to establish low impedance (confirmed as <20 kΩ) between each electrode and the scalp. 64-channels of data, including an ECG channel, were recorded at 10 kHz concurrent with fMRI using an MRI compatible system. Time marks generated by the scanner at the onset of each volume acquisition were used to reduce gradient-related artifacts via an average artifact subtraction method.[47] Heartbeat timings generated from the ECG channel were used to reduce the ballistocardiographic artifact via a linear spatial filtering method.[48] All EEG data were reviewed by a board certified epilepsy specialist (JPS), and GSWD timings were marked to within 10 ms precision.

MRI Acquisition & Processing

Acquisition of MRI and fMRI data was carried out on a 4 Tesla, 61.5 cm bore Varian Unity INOVA system (Varian, Inc., Palo Alto, CA) equipped with a standard head coil.[18,38] T1-weighted structural images were acquired for use as an anatomical reference. A modified driven equilibrium Fourier transform (MDEFT) method was used with an 1100 millisecond inversion delay, 256×196×196 mm field of view, 256×196×196 voxel matrix, 22° flip angle, and TR/TE = 13.1/6.0 ms. T2*-weighted echo-planar functional images with blood oxygenation level-dependent (BOLD) contrast, were acquired with an 256×256 mm field of view, 64×64 voxel matrix, 90° flip angle, and 5 mm slice thickness in axial orientation without gap. 400 volumes consisting of 30 slices each and TR/TA = 3000/2000 ms were collected during each scan.

Data were reconstructed and corrected for geometric distortion and Nyquist ghosting with the aid of multi-echo reference scans (MERS).[49] Functional scans underwent slice timing correction, motion correction, rigid-body registration to a high-resolution anatomical scan, and non-linear registration to an MNI152 standard using FSL.[50] Data were spatially blurred in-mask with a gaussian kernel of FWHM = 6 mm using AFNI.[51] The quality of functional to anatomical registration was measured using the mutual information cost function. Twelve functional scans with an outlying cost indicating unsatisfactory registration were excluded from the study. The quality of motion correction was measured using the normalized correlation ratio cost function of each timepoint to the reference volume. Thirteen additional scans with outlying costs indicating excessive motion were excluded from the study.

Seed-Based Voxel Correlation

Seed selection was guided by a previous study of the same patient cohort in which we identified a set of brain regions with GSWD-related activation that was increased in patients resistant to treatment with valproate.[38] These included a cluster of voxels in midline paracingulate cortex, located functionally between “sensorimotor” and “executive-control” networks.[52] This region was used as an *a priori* seed with its centroid at MNI coordinates X=2.0, Y=13.6, Z=45.9 and a volume of 38 voxels. Two *a posteriori* seeds were manually generated from regions exhibiting high functional connectivity with the *a priori* paracingulate seed. These were bilateral seeds located in dorsal anterior thalamus (X=±9.2, Y=-15.6, Z=13.6, 5 voxels each side, 10 voxels total) and cerebellum (X=±31.6, Y=-56.4, Z=-28.8, 6 voxels each side, 12 voxels total). A second *a priori* seed in the posterior

cingulate cortex (PCC, X=2.0, Y=-58.0, Z=24.0, 19 voxels), a region regarded as a default mode network "hub",[53] was used to investigate DMN connectivity.[18,20]

The mean timecourse of voxels within each seed region was extracted prior to spatial blurring and was then used as the regressor of interest in a general linear model of the spatially blurred fMRI data for each subject (3dDeconvolve tool in AFNI). The output of 3dDeconvolve was submitted to the 3dREMLfit tool in AFNI to achieve temporal prewhitening via an autoregressive (AR) model. Baseline drift was modeled using a first-order polynomial as no physiologic regressors were available. No global or tissue regressors were used because these may introduce an unwanted bias.[54] However, motion has been shown to have an artifactual effect on resting-state connectivity.[55,56] Therefore, we included the six-rigid body motion parameters generated by FSL as nuisance regressors in the model. In addition, timepoints associated with high motion measured as the normalized correlation ratio cost function > 0.00185 to the reference volume were excluded from analysis. Three timepoints were excluded: those preceeding, including, and following each high-motion volume.

We included subjects and scans containing interictal GSWD in our analysis in order to examine the relationship between RSFC and interictal GSWD frequency. To avoid possible contamination of the resting-state by GSWD, timepoints associated with GSWD were excluded from analysis in a manner analagous to the exclusion of high-motion timepoints. A total of 19 timepoints comprising 57 seconds were excluded for each GSWD: the 9 preceding, 9 following, and 1 including the GSWD. The exclusion of timepoints from the general linear model due to GSWD and motion resulted in ill-conditioned design matrices for 2 GGE subjects (5 scans) with very frequent GSWD who were therefore excluded from the study.

Voxelwise Analysis

The Pearson correlation coefficient of each voxel with the seed timecourse was converted to a z-value using the Fisher transformation. Voxelwise analysis of the resultant z-values was carried out using R.[57] GGE patients were divided into two groups: those who had experienced at least one seizure during the 3 months leading up to scanning (Seizures+) and those who were seizure-free (Seizures-). T-maps of connectivity for all GGE patients vs. controls and for GGE patients who were Seizures+ vs. GGE patients who were Seizures- were computed with age[58] and music-listening[46] as covariates. The correlation between connectivity and GSWD-frequency (measured as # GSWD / # scans) in GGE patients was also computed.

Cluster-based correction for multiple comparisons was carried out using the AlphaSim and 3dmerge tools in AFNI at a significance level of α=0.05. Ventricular and white matter masks were generated from the Harvard-Oxford subcortical probabilistic atlas (p>50%) distributed with FSL.[59] Observations within these regions were assumed to be artifactual, therefore t-maps were masked prior to cluster-based thresholding to avoid inflation of cluster sizes by spurious correlations.

Results

GSWD Frequency

GSWD frequency (# GSWD / # scans) was significantly correlated with RSFC in GGE patients for each seed. The most widespread increases in RSFC with GSWD frequency were observed for the paracingulate seed and included the frontal areas of superior frontal, medial frontal, inferior frontal, orbitofrontal, and anterior cingulate cortex (ACC); the posterior areas of precuneus, lingual gyrus, lateral occipital, and posterior cingulate cortex (PCC); and subcortical regions thalamus and basal ganglia. Increased RSFC was also observed in precentral gyrus and posterior cerebellum (Figure 1A). Similar results were obtained for the PCC seed, except that the posterior regions of precuneus, lingual gyrus, and lateral occipital cortex were unchanged (Figure 1B). RSFC with the cerebellar seed increased significantly with spike frequency for ACC, left insula, right thalamus, and posterior cerebellum (Figure 1C). RSFC with the thalamic seed increased significantly with spike frequency for right insula, right thalamus, and left basal ganglia (Figure 1).

The relationship between GSWD frequency and RSFC was also investigated using a seed in PCC,[20] a default mode network (DMN) hub region.[53] Results were similar to those obtained via the paracingulate seed and included significant positive correlations between RSFC and GSWD frequency in precentral gyrus, insula, thalamus, basal ganglia, superior frontal, medial frontal, inferior frontal, orbitofrontal, and anterior cingulate cortex (Figure 1D).

GGE Patients vs. Healthy Controls

No significant difference in corticothalamic RSFC between GGE patients and healthy controls was detected using the a priori paracingulate seed (Figure 2A), but significant changes in thalamocortical RSFC were observed using the *a posteriori* thalamic seed (Figure 2B). RSFC between thalamus and medial frontal cortex (X=-0.7, Y=9.1, Z=55.6, 41 voxels) was significantly greater in GGE patients vs. healthy controls while RSFC between thalamus and posterior cingulate cortex (PCC, X=-0.5, Y=-28.3, Z=30.0, 33 voxels) was significantly reduced.

The *a posteriori* thalamic seed was manually generated from subthreshold (i.e. not-significant) trends in corticothalamic RSFC observed for GGE patients vs. healthy controls observed using the paracingulate seed (Figure 3). GGE patients trended toward greater connectivity between the paracingulate seed and dorsal anterior thalamus than did healthy controls, but they trended toward reduced RSFC between the paracingulate seed and ventral posterior thalamus. See Table 2.

Seizures+ vs. Seizures- Patients

GGE patients with uncontrolled seizures (Seizures+) exhibited significantly reduced RSFC between the paracingulate seed and bilateral cerebellum (X=-32.0, Y=-54.9, Z=-30.3, 36 voxels; X=34.0, Y=-53.7; Z=-26.9, 27 voxels) when compared to the Seizures- GGE patients (Figure 4A). A manually-created *a posteriori* seed in the cerebellum exhibited significantly reduced reciprocal RSFC with the paracingulate seed region in Seizures+ vs.

Seizures- (Figure 4B). The cerebellar seed also exhibited significantly reduced connectivity with thalamus, basal ganglia, and cortex diffusely.

Discussion

GSWD Frequency

We observed significant functional connectivity changes in GGE patients correlated with GSWD frequency despite excluding a generous amount of fMRI data (19 TRs = 57 seconds) around each GSWD detected using simultaneous EEG. The most extensive findings were for the paracingulate seed, which is associated with treatment resistance,[38] and the PCC seed, which measures DMN RSFC.[20] Increased correlations of paracingulate RSFC with GSWD frequency (Figure 1A) were observed in frontal regions associated with attention, anterior insulae[34] and posterior regions associated with the DMN, and subcortical regions. Increased correlations of PCC RSFC with GSWD were also observed in frontal/attentional regions. These findings support the hypothesis that RSFC is altered in brains with frequent GSWD activity. Executive networks, especially the DMN, appear to be the most affected, consistent with reduced DMN connectivity[18,19,20] and executive function[13,5,6,14,12,7,8,15] in GGE patients. Paracingulate RSFC with precentral gyrus was correlated with GSWD frequency (Figure 1A). This finding could be an artifact of the analysis, as the paracingulate seed is located functionally on the border of motor cortex.[52] However, paracingulate RSFC was correlated with GSWD frequency for thalamus and basal ganglia as well, subcortical regions that support both motor and executive functions. Thus, the involvement of precentral gyrus could alternatively be interpreted as evidence for increased crosstalk between motor, default mode, and executive networks in patients with frequent GSWDs.

GGE Patients vs. Healthy Controls

Whereas GSWDs are associated with widespread cortical activation, we found evidence for increased thalamocortical RSFC only in medial frontal cortex (Figure 2B). This is consistent with the so-called “cortical focus” hypothesis that specific cortical regions (i.e. medial frontal cortex) sustain reentrant activity in thalamocortical ictogenic circuits.[60,61,38] However, this finding is equivocal because significant changes in thalmocortical RSFC were found using the *a posteriori* thalamic (Figure 2B), but not *a priori* paracingulate (Figure 2A), seed and could thus have been biased by manual seed selection (i.e. “seed-fishing”).

Despite considerable evidence for the thalamocortical hypothesis of GSWD, changes in thalamocortical connectivity are not consistently observed using MRI.[21] Significance in fMRI is often determined using cluster-based thresholding, which required at least 26 suprathreshold voxels in our analysis. Anatomically, there are 36 voxels in each thalamic hemisphere (Harvard-Oxford Subcortical Atlas, probability > 90%)[59] at our imaging resolution. Therefore, implicit in our analysis is the assumption that at least 26/36 = 72% of thalamus is affected the same way by GGE. However, in Figure 3 we observe positive and negative clusters of subthreshold changes in RSFC that divide the thalamus roughly in half. Although the findings in Figure 3 are based on subthreshold analyses, they are consistent with previous studies in which thalamic nuclei are affected differently by epilepsy,[62] exhibit different, and even opposite, connectivity changes in epilepsy,[22] and play different roles in

the initiation vs. maintenance of seizure activity.[39] Therefore, the statistical power to detect thalamic changes in RSFC associated with GGE is limited in our and potentially other fMRI studies.

Seizures+ vs. Seizures- Patients

At least two previous EEG/fMRI studies have discussed inconclusive cerebellar findings in GGE.[28,21] The cerebellum shares reciprocal connections with thalamus, cortex,[63] and basal ganglia[64] through which it could, theoretically, modulate ictogenic activity throughout the brain. Paracingulate RSFC in Seizures+ vs. Seizures- was significantly reduced exclusively with cerebellum (Figure 4A), however the same relationship was not observed for GGE patients vs. controls (Figure 2A). Reciprocal cerebellar RSFC was reduced in thalamus, basal ganglia, and most of cortex for Seizures+ vs. Seizures-(Figure 4B). Although cerebellum is not thought to be a primary cause of ictogenesis in GGE, these data suggest that loss of cerebellar connectivity with thalamus, basal ganglia, and cortex is associated with seizures resistant to treatment. Prospective studies would be needed to establish causality and rule out confounding effects of AED treatment.

Acknowledgments

This study was supported in part by a grant from the National Institute of Neurological Disorders and Stroke (K23 NS052468) and in part by funds from the Department of Neurology at the University of Cincinnati Academic Health Center, Cincinnati, OH, USA. The first author received support from the Medical Scientist Training Program (MSTP) at the University of Cincinnati (T32 GM063483).

References

1. Berg AT, Berkovic SF, Brodie MJ, et al. Revised terminology and concepts for organization of seizures and epilepsies: report of the ILAE Commission on Classification and Terminology, 2005-2009. Epilepsia. 2010; 51:676–85. [PubMed: 20196795]
2. Jallon P, Latour P. Epidemiology of idiopathic generalized epilepsies. Epilepsia. 2005; 46:10–4. [PubMed: 16302871]
3. Faught E. Treatment of refractory primary generalized epilepsy. Rev Neurol Dis. 2004; 1:S34–43. [PubMed: 16400293]
4. Gelisse P, Genton P, Thomas P, et al. Clinical factors of drug resistance in juvenile myoclonic epilepsy. J Neurol Neurosurg Psychiatry. 2001; 70:240–3. [PubMed: 11160477]
5. Devinsky O, Gershengorn J, Brown E, et al. Frontal functions in juvenile myoclonic epilepsy. Neuropsychiatry Neuropsychol Behav Neurol. 1997; 10:243–6. [PubMed: 9359121]
6. Iqbal N, Caswell HL, Hare DJ, et al. Neuropsychological profiles of patients with juvenile myoclonic epilepsy and their siblings: a preliminary controlled experimental video-EEG case series. Epilepsy Behav. 2009; 14:516–21. [PubMed: 19166970]
7. Kim SY, Hwang YH, Lee HW, et al. Cognitive impairment in juvenile myoclonic epilepsy. J Clin Neurol. 2007; 3:86–92. [PubMed: 19513297]
8. Kim JH, Suh SI, Park SY, et al. Microstructural white matter abnormality and frontal cognitive dysfunctions in juvenile myoclonic epilepsy. Epilepsia. 2012; 53:1371–8. [PubMed: 22708960]
9. Mula M, Trimble MR. Antiepileptic drug-induced cognitive adverse effects: potential mechanisms and contributing factors. CNS Drugs. 2009; 23:121–37. [PubMed: 19173372]
10. Szaflarski JP, Allendorfer JB. Topiramate and its effect on fMRI of language in patients with right or left temporal lobe epilepsy. Epilepsy Behav. 2012; 24:74–80. [PubMed: 22481042]
11. Yasuda CL, Centeno M, Vollmar C, et al. The effect of topiramate on cognitive fMRI. Epilepsy Res. 2013; 105:250–5. [PubMed: 23333471]

12. Killory BD, Bai X, Negishi M, et al. Impaired attention and network connectivity in childhood absence epilepsy. Neuroimage. 2011; 56:2209–17. [PubMed: 21421063]
13. Akanuma N, Hara E, Adachi N, et al. Psychiatric comorbidity in adult patients with idiopathic generalized epilepsy. Epilepsy Behav. 2008; 13:248–51. [PubMed: 18353731]
14. Jones NC, Salzberg MR, Kumar G, et al. Elevated anxiety and depressive-like behavior in a rat model of genetic generalized epilepsy suggesting common causation. Exp Neurol. 2008; 209:254–60. 2008. [PubMed: 18022621]
15. Trinka E, Kienpointner G, Unterberger I, et al. Psychiatric comorbidity in juvenile myoclonic epilepsy. Epilepsia. 2006; 47:2086–91. [PubMed: 17201708]
16. Greicius MD, Supekar K, Menon V, et al. Resting-state functional connectivity reflects structural connectivity in the default mode network. Cereb Cortex. 2009; 19:72–8. [PubMed: 18403396]
17. Zhang Z, Liao W, Chen H, et al. Altered functional-structural coupling of large-scale brain networks in idiopathic generalized epilepsy. Brain. 2011; 134:2912–28. [PubMed: 21975588]
18. Kay BP, Difrancesco MW, Privitera MD, et al. Reduced default mode network connectivity in treatment-resistant idiopathic generalized epilepsy. Epilepsia. 2013; 54:461–470. [PubMed: 23293853]
19. Luo C, Li Q, Lai Y, et al. Altered functional connectivity in default mode network in absence epilepsy: a resting-state fMRI study. Hum Brain Mapp. 2011; 32:438–49. [PubMed: 21319269]
20. McGill ML, Devinsky O, Kelly C, et al. Default mode network abnormalities in idiopathic generalized epilepsy. Epilepsy Behav. 2012; 23:353–9. [PubMed: 22381387]
21. Moeller F, Maneshi M, Pittau F, et al. Functional connectivity in patients with idiopathic generalized epilepsy. Epilepsia. 2011; 52:515–22. [PubMed: 21269293]
22. O'Muircheartaigh J, Vollmar C, Barker GJ, et al. Abnormal thalamocortical structural and functional connectivity in juvenile myoclonic epilepsy. Brain. 2012; 135:3635–44. [PubMed: 23250883]
23. Yenjun S, Harvey AS, Marini C, et al. EEG in adult-onset idiopathic generalized epilepsy. Epilepsia. 2003; 44:242–6.
24. Szaflarski JP, Lindsell CJ, Zakaria T, et al. Seizure control in patients with idiopathic generalized epilepsies: EEG determinants of medication response. Epilepsy Behav. 2010; 17:525–30. [PubMed: 20227351]
25. Blumenfeld H. The thalamus and seizures. Arch Neurol. 2002; 59:135–7. [PubMed: 11790241]
26. Contreras D, Destexhe A, Sejnowski TJ, et al. Control of spatiotemporal coherence of a thalamic oscillation by corticothalamic feedback. Science. 1996; 274:771–4. [PubMed: 8864114]
27. Moeller F, Siebner HR, Wolff S, et al. Changes in activity of striato-thalamo-cortical network precede generalized spike wave discharges. Neuroimage. 2008; 39:1839–49. [PubMed: 18082429]
28. Blumenfeld H. Cellular and network mechanisms of spike-wave seizures. Epilepsia. 2005; 46:S21–33.
29. Destexhe A. Spike-and-wave oscillations based on the properties of GABAB receptors. J Neurosci. 1998; 18:9099–111. [PubMed: 9787013]
30. Coenen AM, Van Luijtelaar EL. Genetic animal models for absence epilepsy: a review of the WAG/Rij strain of rats. Behav Genet. 2003; 33:635–55. [PubMed: 14574120]
31. Engel, J, Jr.. Surgical Treatment of the Epilepsies. 2nd Edition. Raven Press; New York: 1993. Chapters 9-10
32. Gotman J, Kobayashi E, Bagshaw AP, et al. Combining EEG and fMRI: a multimodal tool for epilepsy research. J Magn Reson Imaging. 2006; 23:906–20. [PubMed: 16649203]
33. Aghakhani Y, Bagshaw AP, Bénar CG, et al. fMRI activation during spike and wave discharges in idiopathic generalized epilepsy. Brain. 2004; 127:1127–44. 2004. [PubMed: 15033899]
34. Gotman J, Grova C, Bagshaw A, et al. Generalized epileptic discharges show thalamocortical activation and suspension of the default state of the brain. Proc Natl Acad Sci U S A. 2005; 102:15236–40. [PubMed: 16217042]
35. Hamandi K, Salek-Haddadi A, Laufs H, et al. EEG-fMRI of idiopathic and secondarily generalized epilepsies. Neuroimage. 2006; 31:1700–10. [PubMed: 16624589]

36. Moeller F, Siebner HR, Wolff S, et al. Simultaneous EEG-fMRI in drug-naive children with newly diagnosed absence epilepsy. Epilepsia. 2008; 49:1510–9. [PubMed: 18435752]
37. Szaflarski JP, DiFrancesco MW, Hirschauer T, et al. Cortical and subcortical contributions to absence seizure onset examined with EEG/fMRI. Epilepsy Behav. 2010; 18:404–13. [PubMed: 20580319]
38. Szaflarski JP, Kay B, Gotman J, et al. The relationship between the localization of the generalized spike and wave discharge generators and the response to valproate. Epilepsia. 2013; 54:471–480. [PubMed: 23294001]
39. Tyvaert L, Chassagnon S, Sadikot A, et al. Thalamic nuclei activity in idiopathic generalized epilepsy: an EEG-fMRI study. Neurology. 2009; 73:2018–22. [PubMed: 19996076]
40. Fox MD, Snyder AZ, Vincent JL, et al. The human brain is intrinsically organized into dynamic, anticorrelated functional networks. Proc Natl Acad Sci U S A. 2005; 102:9673–8. [PubMed: 15976020]
41. Morgan VL, Gore JC, Szaflarski JP. Temporal clustering analysis: what does it tell us about the resting state of the brain? Med Sci Monit. 2008; 14:CR345–52. [PubMed: 18591915]
42. Raichle ME, MacLeod AM, Snyder AZ, et al. A default mode of brain function. Proc Natl Acad Sci U S A. 2001; 98:676–82. [PubMed: 11209064]
43. Vanhaudenhuyse A, Noirhomme Q, Tshibanda LJ, et al. Default network connectivity reflects the level of consciousness in non-communicative brain-damaged patients. Brain. 2010; 133:161–71. [PubMed: 20034928]
44. Danielson NB, Guo JN, Blumenfeld H. The default mode network and altered consciousness in epilepsy. Behav Neurol. 2011; 24:55–65. [PubMed: 21447899]
45. Vaudano AE, Laufs H, Kiebel SJ, et al. Causal hierarchy within the thalamo-cortical network in spike and wave discharges. PLoS One. 2009; 4:e6475. [PubMed: 19649252]
46. Kay BP, Meng X, Difrancesco MW, et al. Moderating effects of music on resting state networks. Brain Res. 2012; 1447:53–64. [PubMed: 22365746]
47. Allen PJ, Josephs O, Turner R. A method for removing imaging artifact from continuous EEG recorded during functional MRI. Neuroimage. 2000; 12:230–9. [PubMed: 10913328]
48. Lagerlund TD, Sharbrough FW, Busacker NE. Spatial filtering of multichannel electroencephalographic recordings through principal component analysis by singular value decomposition. J Clin Neurophysiol. 1997; 14:73–82. [PubMed: 9013362]
49. Schmithorst VJ, Dardzinski BJ, Holland SK. Simultaneous correction of ghost and geometric distortion artifacts in EPI using a multiecho reference scan. IEEE Trans Med Imaging. 2001; 20:535–9. [PubMed: 11437113]
50. Smith SM, Jenkinson M, Woolrich MW, et al. Advances in functional and structural MR image analysis and implementation as FSL. Neuroimage. 2004; 23:S208–19. [PubMed: 15501092]
51. Cox RW. AFNI: software for analysis and visualization of functional magnetic resonance neuroimages. Comput Biomed Res. 1996; 29:162–73. [PubMed: 8812068]
52. Smith SM, Fox PT, Miller KL, et al. Correspondence of the brain's functional architecture during activation and rest. Proc Natl Acad Sci U S A. 2009; 106:13040–5. [PubMed: 19620724]
53. Greicius MD, Krasnow B, Reiss AL, et al. Functional connectivity in the resting brain: a network analysis of the default mode hypothesis. Proc Natl Acad Sci U S A. 2003; 100:253–8. [PubMed: 12506194]
54. Weissenbacher A, Kasess C, Gerstl F, et al. Correlations and anticorrelations in resting-state functional connectivity MRI: a quantitative comparison of preprocessing strategies. Neuroimage. 2009; 47:1408–16. [PubMed: 19442749]
55. Power JD, Barnes KA, Snyder AZ, et al. Spurious but systematic correlations in functional connectivity MRI networks arise from subject motion. Neuroimage. 2012; 59:2142–54. [PubMed: 22019881]
56. Van Dijk KR, Sabuncu MR, Buckner RL. The influence of head motion on intrinsic functional connectivity MRI. Neuroimage. 2012; 59:431–8. [PubMed: 21810475]
57. Whitcher B, Schmid VJ, Thornton A. Working with the DICOM and NIfTI Data Standards in R. J Stat Softw. 2011; 44:1–28.

58. Ferreira LK, Busatto GF. Resting-state functional connectivity in normal brain aging. Neurosci Biobehav Rev. 2013; 37:384–400. [PubMed: 23333262]

59. Desikan RS, Ségonne F, Fischl B, et al. An automated labeling system for subdividing the human cerebral cortex on MRI scans into gyral based regions of interest. Neuroimage. 2006; 31(3):968–80. [PubMed: 16530430]

60. Meeren H, van Luijtelaar G, Lopes da Silva F, et al. Evolving concepts on the pathophysiology of absence seizures: the cortical focus theory. Arch Neurol. 2005; 62:371–6. [PubMed: 15767501]

61. Niedermeyer E. Primary (idiopathic) generalized epilepsy and underlying mechanisms. Clin Electroencephalogr. 1996; 27(1):1–21. [PubMed: 8719497]

62. Betting LE, Mory SB, Li LM, et al. Voxel-based morphometry in patients with idiopathic generalized epilepsies. Neuroimage. 2006; 32:498–502. [PubMed: 16702001]

63. Ramnani N. The primate cortico-cerebellar system: anatomy and function. Nat Rev Neurosci. 2006; 7:511–22. [PubMed: 16791141]

64. Bostan AC, Dum RP, Strick PL. The basal ganglia communicate with the cerebellum. Proc Natl Acad Sci U S A. 2010; 107:8452–6. [PubMed: 20404184]

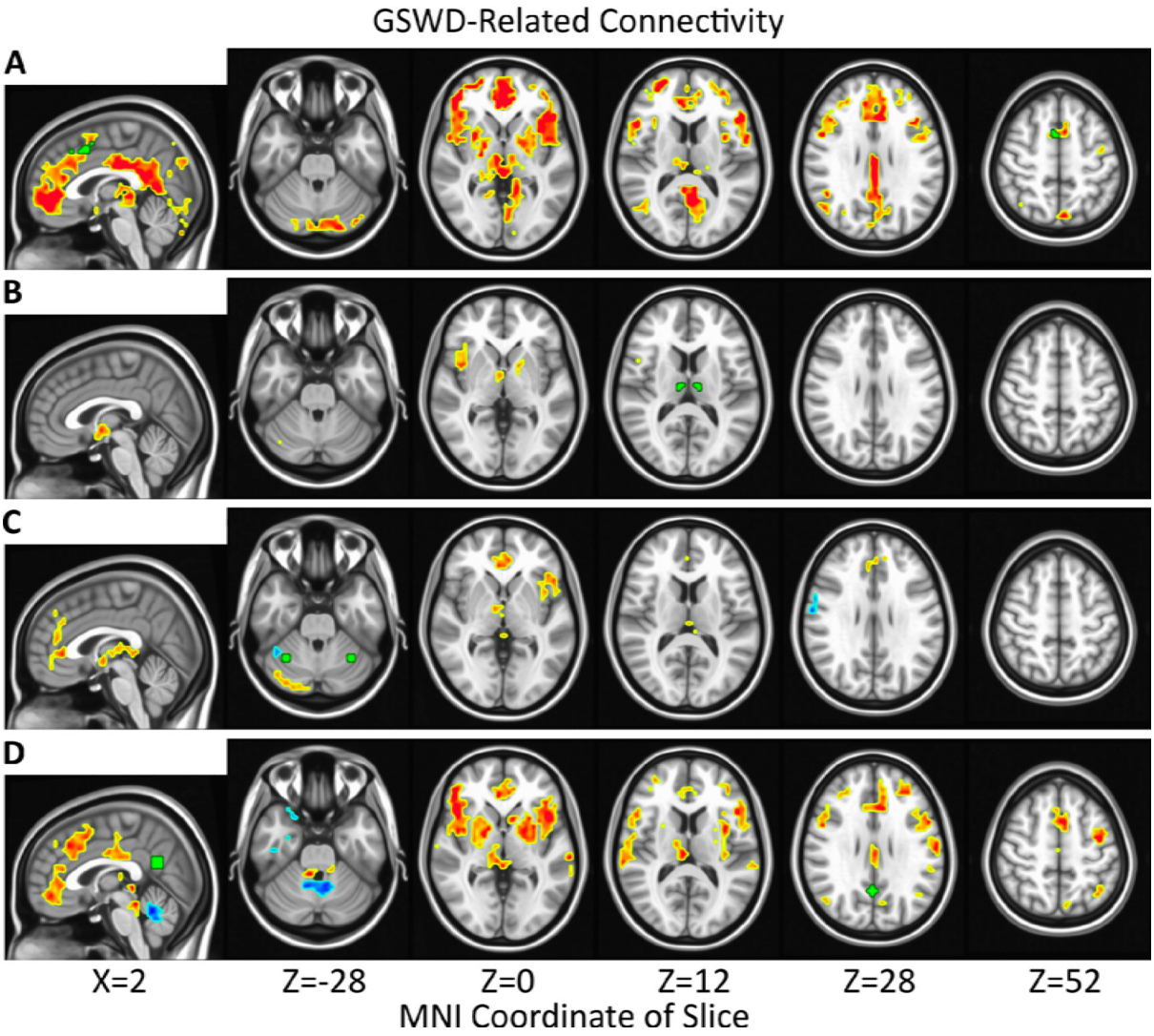

Figure 1.

Significantly (α=0.05, $|t|>2.24$, $p<0.043$, # voxels≥40) increased (red) and decreased (blue) correlations of connectivity with spike frequency (# GSWD/# scans) in epilepsy patients are overlayed on the MNI152 standard brain in radiological orientation. Seed regions are shown in green for paracingulate cortex (**A**), thalamus (**B**), cerebellum (**C**), and posterior cingulate cortex (**D**).

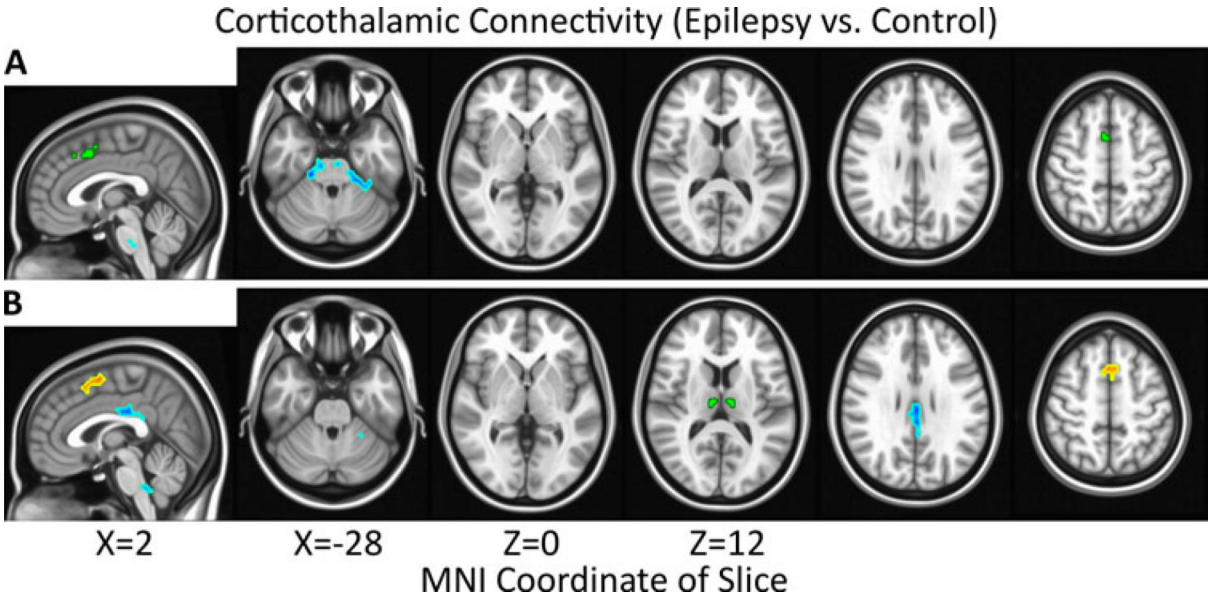

Figure 2.

Significant (α=0.05, $|t|>2.24$, $p<0.027$, # voxels$\geq$26) increases (red) and decreases (blue) in connectivity for epilepsy patients vs. healthy controls are overlayed on the MNI152 standard brain in radiological orientation. Seed regions are shown in green for paracingulate cortex (**A**) and thalamus (**B**).

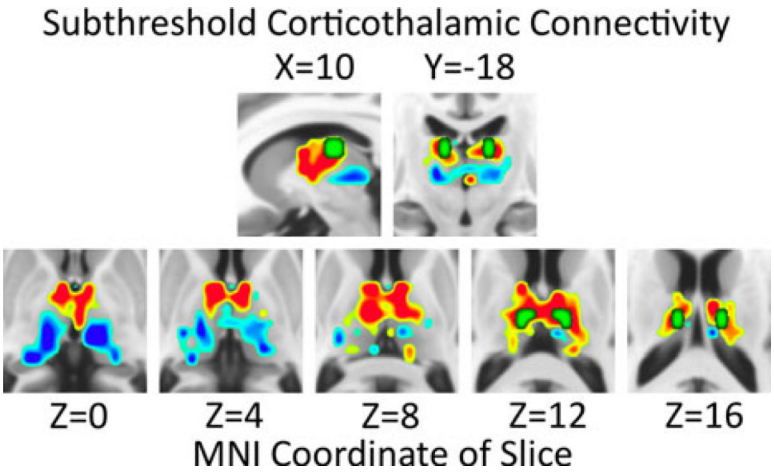

Figure 3.

Increases (red) and decreases (blue) in connectivity between the paracingulate seed region and thalamus for epilepsy patients vs. healthy controls are overlayed on the MNI152 standard brain in radiological orientation. The paracingulate seed region is not shown but is labeled in green in Figures 1A, 2A, and 4A. The manually-generated thalamic seed region is shown in green. All voxels with $|t|>0.25$ are shown, including those below the threshold for statistical significance ($\alpha=0.05$).

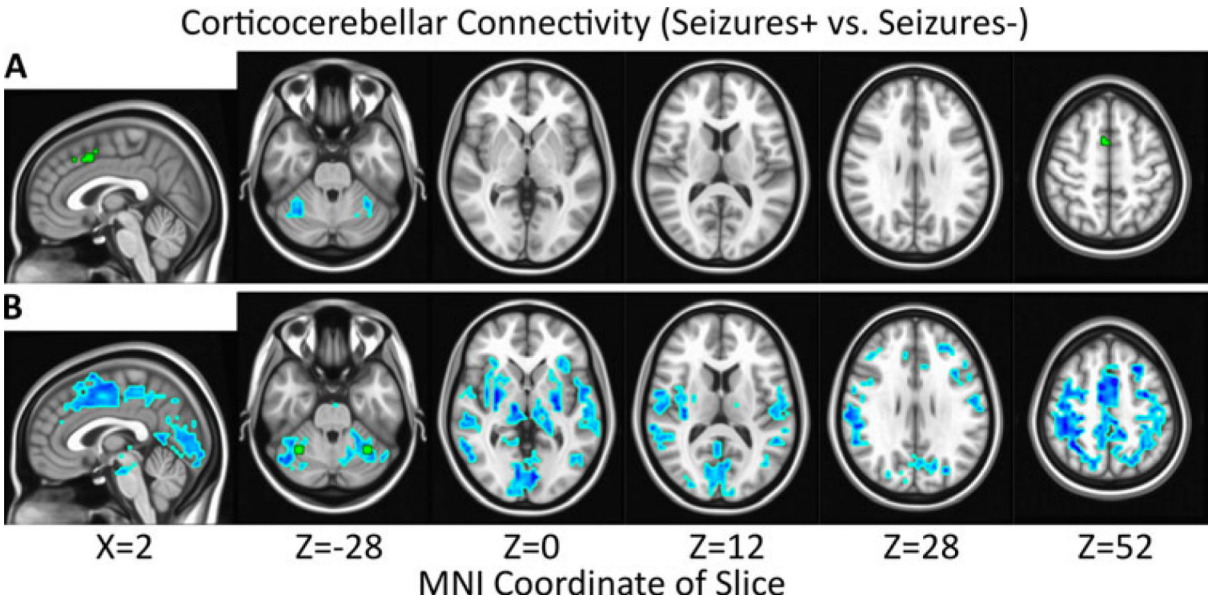

Figure 4.

Significant (α=0.05, |t|>2.24, p<0.028, # voxels≥27) decreases (blue) in connectivity for epilepsy patients with uncontrolled seizures (Seizures+) vs. seizure-free patients (Seizures-) are overlayed on the MNI152 standard brain in radiological orientation. Seed regions are shown in green for paracingulate cortex (**A**) and cerebellum (**B**).

Table 1

Demographics of generalized generalized epilepsy (GGE) patients, subdivided by clinical feature, and healthy controls.

	# Runs	# Males	# Females	Age (years±SD)	Duration (years±SD)	# Current Drugs	# Failed Drugs
GGE (All)	**152**	**32**	**40**	**31.3±11.5**	**14.5±11.4**	**1.50**	**2.05**
GGE (Seizures−)	107	19	30	32.3±10.9	14.9±10.7	1.29	1.47
GGE (Seizures+)	45	13	10	29.1±12.6	13.6±13.1	1.96	3.30
GGE (GSWD−)	108	18	31	31.9±11.3	14.9±10.5	1.33	1.76
GGE (GSWD+)	44	14	9	29.9±12.1	13.6±13.4	1.87	2.70
GGE (JME)	73	18	18	27.8±8.8	13.2±9.0	1.44	2.25
GGE (Other)	79	14	22	34.8±12.9	15.8±13.4	1.56	1.86
Control	**67**	**22**	**16**	**30.9±10.2**			

Mean age and duration of epilepsy at scanning (± standard deviation) are given in years. Seizures− = epilepsy patients who were seizure-free during the three months leading up to scanning. Seizures+ = GGE patients who experienced at least one seizure during the three months leading up to scanning. JME = juvenile myoclonic epilepsy.

Table 2

Subthreshold (|t|>0.25) clusters of thalamic connectivity with the paracingulate seed in GGE patients vs. healthy controls.

Side	Sign	X	Y	Z
Left	+	−7.8	−12.4	9.0
Left	−	−10.6	−23.8	3.5
Right	+	8.5	−11.4	8.7
Right	−	13.7	−24.2	2.5

The thalamic hemisphere (left vs. right side), sign (increased vs. decreased connectivity), and MNI coordinates (X,Y,Z) are given. See Figure 3.